Low Energy Electrodynamics of CrI3 Layered Ferromagnet

Luca Tomarchio
Sapienza University of Rome
Salvatore Macis
Sapienza University of Rome
Lorenzo Mosesso
Sapienza University of Rome
Loi T. Nguyen
Princeton University
Antonio Grilli
National Laboratory of Frascati
Mariangela Cestelli Guidi
National Laboratory of Frascati
Robert J. Cava
Princeton University
Stefano Lupi (stefano.lupi@uniroma1.it)
Sapienza University of Rome

Research Article

Keywords: Low Energy Electrodynamics, CrI3, Ferromagnet, terahertz (THz), Near-Infrared (NIR), Three-dimensional (3D)

Posted Date: July 24th, 2021

DOI: https://doi.org/10.21203/rs.3.rs-732107/v1

Version of Record: A version of this preprint was published at Scientific Reports on December 1st, 2021.
See the published version at https://doi.org/10.1038/s41598-021-02918-4.

Low Energy Electrodynamics of CrI_3 Layered Ferromagnet

Luca Tomarchio [1,2], Salvatore Macis [1,3], Lorenzo Mosesso,[1] Loi T. Nguyen,[4] Antonio Grilli,[3] Mariangela Cestelli Guidi [3], Robert J. Cava,[4] and Stefano Lupi[1,3,*]

[1] *Department of Physics, Sapienza University, Piazzale Aldo Moro 5, 00185, Rome, Italy.*
[2] *INFN section of Rome, P.Le Aldo Moro, 2, 00185 Rome, Italy.*
[3] *INFN - Laboratori Nazionali di Frascati, via Enrico Fermi 54, 00044, Frascati (Rome), Italy.*
[4] *Department of Chemistry, Princeton University, Princeton, NJ 08544, USA.*

(Dated: July 21, 2021)

We report on the optical properties from terahertz (THz) to Near-Infrared (NIR) of the layered magnetic compound CrI_3 at various temperatures, both in the paramagnetic and ferromagnetic phase. In the NIR spectral range, we have observed an insulating electronic gap around 1.1 eV which strongly hardens with decreasing temperature. The blue shift observed represents a record in insulating materials and it is a fingerprint of a strong electron-phonon interaction. Moreover, a further gap hardening is observed below the Curie temperature, indicating the establishment of an effective interaction between electrons and magnetic degrees of freedom in the ferromagnetic phase. This interaction is confirmed by the disappearance of some phonon modes in the same phase as expected from a spin-lattice interaction theory. Therefore, the optical properties of CrI_3 reveal a complex interaction among electronic, phononic and magnetic degrees of freedom, opening many possibilities for its use in 2-Dimensional heterostructures.

PACS numbers:

I. INTRODUCTION

Three-dimensional (3D) layered van der Waals (vdW) crystals[1–3] are systems preserving the 2-Dimensional (2D) phenomenology while guaranteeing significant advantages over their applications in 3D bulk devices[4–6]. Their emerging functional properties are associated with non conventional electronic behaviors like excitonic interactions and dynamics[7] and spin/valley physics[8,9]. Recently, these exotic electronic properties combined with intrinsic ferromagnetic order has been found in vdW transition metal halides like CrI_3 and $CrCl_3$[10–15]. Here, ferromagnetism may sustain novel phases of matter, like the Quantum Hall Effect (QHA)[16,17] or the spin liquid state[18,19], opening numerous opportunities for magneto-optical applications[20–22]. Moreover, bulk layered vdW magnets can be exploited as substrates, interfacial layers and tunnel barriers for engineering magnetic proximity effects and designing novel spintronic applications[23,24].

Chromium trihalide CrI_3 has been shown to be a cleavable magnetic material with a great tunability of its magnetic properties with thickness[25–27]. Bulk CrI_3 is a layered c-axis anisotropic ferromagnetic insulator with a Curie temperature of 61 K and a rhombohedral layer stacking below ∼220 K, where a first order structural phase transition converts the unit cell from a monoclinic room temperature phase[28]. In each layer, the Cr atoms form a honeycomb structure (Fig. 1a), with each of them surrounded by six Iodine atoms in an octahedral coordination[25]. Remarkably, few-layer CrI_3 has been proved to host anti-ferromagnetic order between the layers, with a Néel critical temperature of 45 K and a monoclinic stacking[26].

CrI_3 has been theoretically predicted[29,30] to host strong interactions among electronic, phononic and magnetic degrees of freedom, including a strong spin-orbit coupling (SOC)[31–33], with the appearance of exotic responses like nonreciprocal magneto-electric effects[24,34,35]. As a result, CrI_3 is a candidate material to host subtle, low energy, emergent phases of matter[36,37]. Indeed, recent results[38–40] have proved how an isostructural compound like α-$RuCl_3$ is able to host low energy fractionalized excitations reminiscent of a Kitaev spin liquid phase. Moreover, neutron magnetic scattering measurements on CrI_3[41] have suggested the presence of topological magnon dispersions[42], with the appearance of magnon edge states, analogous to topological insulators for electronic systems. Additional studies on the magnetic order revealed how the breaking of the spin-rotation invariance may be caused by large SOC, rather than the crystal field anisotropy[32]. All these results lead to a very complex picture of all degrees of freedom interactions in CrI_3.

Although theoretical and experimental data suggest CrI_3 to be a candidate material for hosting subtle, low energy, emergent phases of matter, its low-energy electronic and vibrational properties have never been investigated, at least in our knowledge. In this work we address the low energy electrodynamics of a CrI_3 single crystal, investigating its optical properties over a broad range of frequencies, going from THz to near infrared (NIR), while tuning the temperature across the structural and magnetic phase transitions, down to the liquid helium temperature. The NIR response of CrI_3 shows the presence of an optical gap associated to the crystal-field splitting of the Cr d-bands (d_{xy,x_2-y_2} and $d_{xz,yz}$)[28,43], which

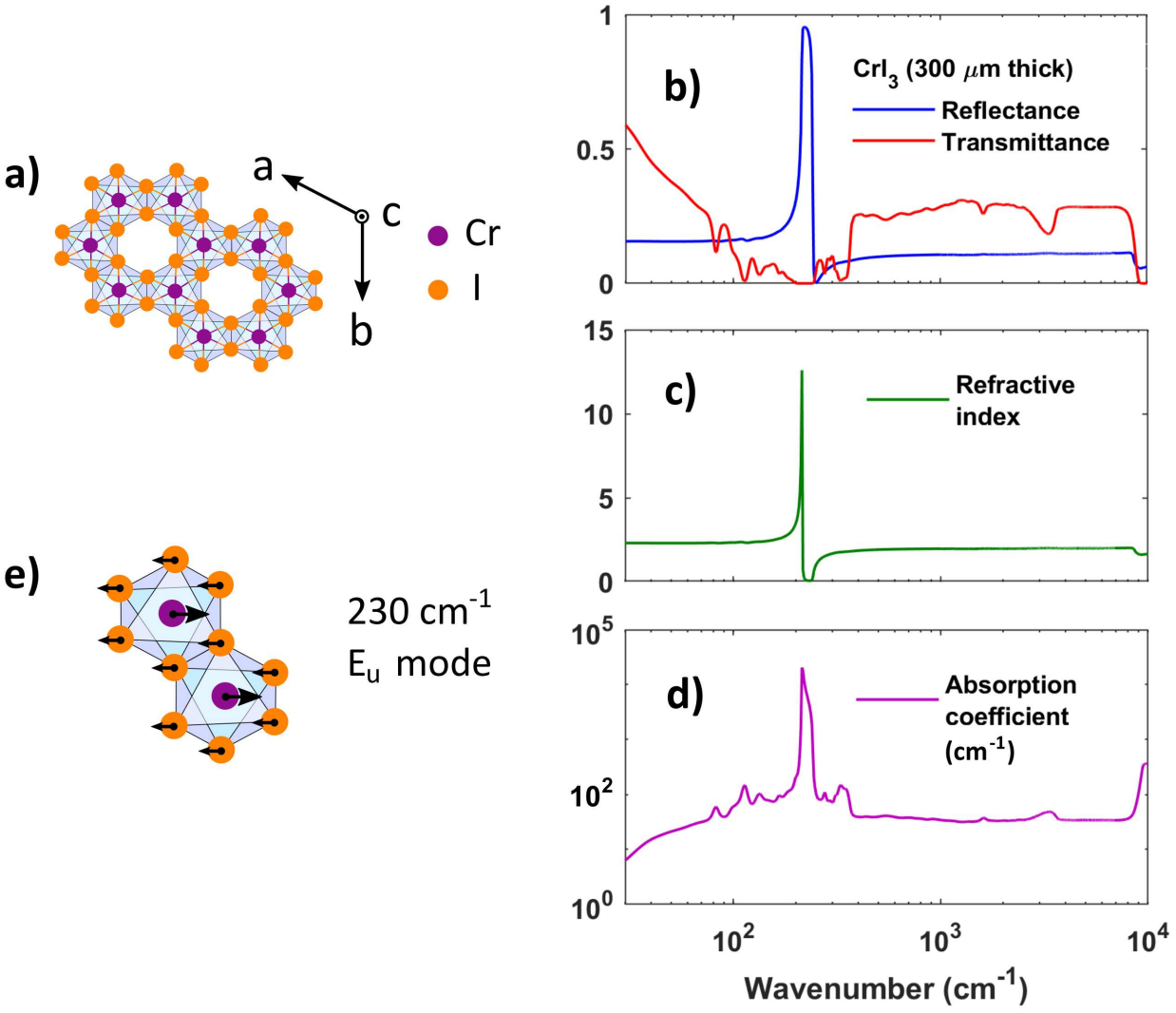

FIG. 1: | **Infrared spectroscopy measurements of a CrI_3 single crystal. a)** Top view of the crystal structure of CrI_3. The Cr and I atoms are bonded to form honeycomb ordered layers. The arrows indicate the crystal axes. **b)** Optical reflectance and transmittance of a 300 μm thick CrI_3 crystal at 300 K. The reflectance is dominated by a single phonon mode at 230 cm^{-1}. The measured transmittance highlights instead a plethora of far infrared vibrational modes and a band-gap around 9200 cm^{-1}. **c)** Real part of the refractive index of CrI_3 at 300 K. **d**) Absorption coefficient at 300 K of CrI_3. **e** In-plane phonon mode of the Cr atoms, associated to the strong vibrational mode at 230 cm^{-1} in the bulk CrI_3.

is subjected to a giant frequency blue shift (nearly 2000 cm^{-1}), from 300 K to 5 K. Although this giant hardening is mainly related to a strong electron-phonon interaction, a further blue shift is observed below the ferromagnetic temperature, also suggesting a strong coupling among electronic and magnetic degrees of freedom. In the far infrared, we show the presence of single and multiple-phonon excitations superimposed to a broad absorption background. We have studied the temperature dependence of these excitations and their modification with the appearance of a magnetic order.

II. RESULTS AND DISCUSSION

CrI_3 single crystals were synthesized by a chemical vapor transport technique (see Methods). The crystal structure of CrI_3 is shown in Fig. 1a. The Chromium (Cr) and Iodine (I) atoms are bonded to form honeycomb ordered layers. The arrows indicate the a, b and c crystal axes. The bulk crystal structure of CrI_3 at room temperature is described by a monoclinic (space group C2/m) unit cell. Below the structural phase transition at $T_{struc} \sim 220$ K, this changes to a rhombohedral symmetry (space group $R\bar{3}$)[28].

Reflectance (R) and Transmittance (T) measurements

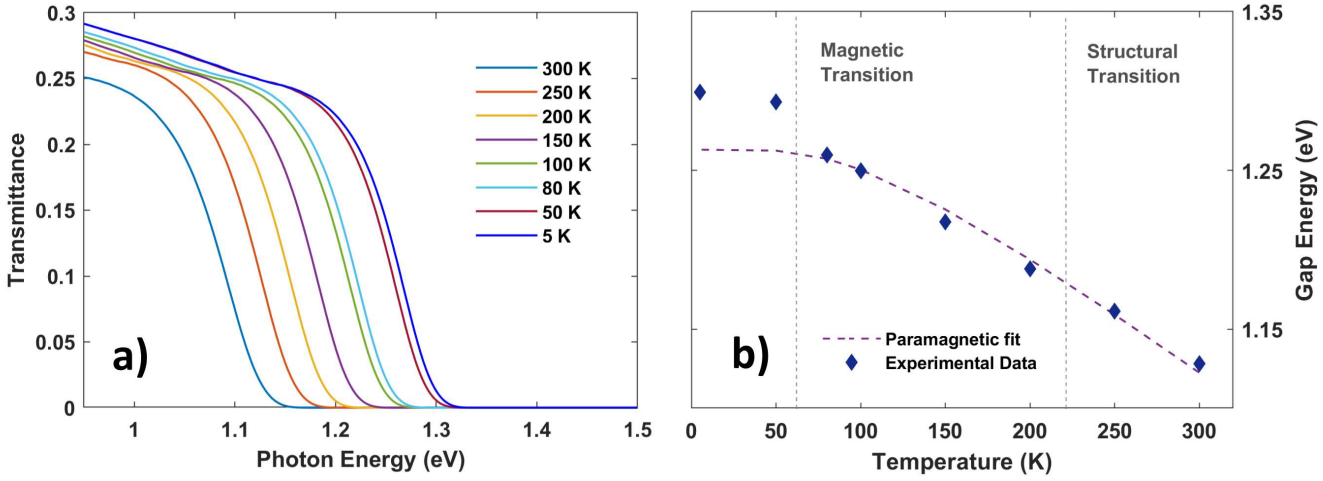

FIG. 2: | **Modulation of the crystal-field electronic band gap of CrI_3 with temperature.** **a)** Measured NIR transmittance for a 300 μm CrI_3 slab at various temperatures. A strong red shift towards higher temperatures is clearly visible. **b)** Optical band-gap as a function of temperature. The dotted line at 61 K separates the values above and below the Curie temperature, where a discontinuity in the band gap energy shift is highlighted. The paramagnetic phase has been fitted through the model in eq. 1, proving the presence of strong electron-phonon correlations in CrI_3 (see table I).

have been performed in a broad spectral range from THz (20 cm^{-1}) to NIR (15000 cm^{-1}) ($\sim$ 2.5 meV – 1.86 eV) and temperatures from 5 to 300 K. The spectroscopy setup is discussed in the Methods section. In Fig. 1b we report the room temperature R and T of a CrI_3 single crystal with a 300 μm thickness. Fig. 1c shows the real part of the refraction index, while Fig. 1d the corresponding absorption coefficient, both extracted through the Ref-Fit Kramers-Kronig consistent fitting process[44]. The reflectance spectrum is dominated by a strong phonon absorption near 230 cm^{-1}, which can be associated to the in-plane E_u collective oscillations of Cr atoms[29] (see Fig. 1e). In the far-infrared transmittance, we are instead able to resolve additional low energy absorption peaks, extending to nearly 400 cm^{-1} which are related to multi-phonon excitations (see below). Above 400 cm^{-1}, a flat transmittance (absorbance) is observed, extending up to the crystal-field electronic gap that can be observed both in transmittance and reflectance at room-T around 9200 cm^{-1} (1.14 eV). The transmittance minima (broad weak maxima in the absorption coefficient, Fig. 1d), appearing on the IR plateau at about 1600 and 3600 cm^{-1}, are instead associated to the bending and stretching vibrations of few intercalated water molecules among the CrI_3 layers[45]. Indeed, layered systems are common hosting materials for various intercalant species, ranging from small ions to atoms and molecules[46].

A. Temperature Dependence of the Electronic Gap

The temperature dependent transmittance measurements in the NIR spectral region are highlighted in Fig. 2a. Here, a huge blue shift (nearly 2000 cm^{-1}) of the electronic gap E_g can be observed with decreasing temperature from 300 K to 5 K. E_g(T) values are extracted by a linear fitting of the decreasing transmittance through its intercept with the frequency axis[47]. E_g(T) as a function of temperature is reported in Fig. 2b. In this Figure, both the ferromagnetic Curie temperature T_c and the structural transition temperature T_{struc} have been indicated by vertical dotted lines. While across the structural transition the electronic gap presents a smooth behavior, at the paramagnetic/ferromagnetic transition, a discontinuity appears with a robust increase in the gap value below T_c. Both the lattice expansion and the electron-phonon interaction may induce a temperature dependence of the electronic gap[48,49]. Both terms can be modeled through the Manoogian and Leclerc empirical equation[48,50]

$$E_g(T) = E_g(T=0) + UT^s - \quad (1)$$

$$-V\epsilon\left(\coth(\epsilon/2k_BT) - 1\right)$$

where U, s, V and ϵ are temperature independent coefficients. U and V are the coupling constants weighting the lattice expansion and electron-phonon interaction contributions, respectively, while ϵ is an energy averaging all the acoustic and optical phonons. E_g data in Fig. 2b for the paramagnetic phase have been fitted through Eq. 1. The result is shown in Fig. 2b through a dashed black line. Fitting coefficients in Eq. 1 are presented in Table I, compared to other semiconductors from literature. The lattice expansion, parametrized by U, has been found to give a negligible contribution to the temperature dependence of E_g. The strongest effect is thus given by the

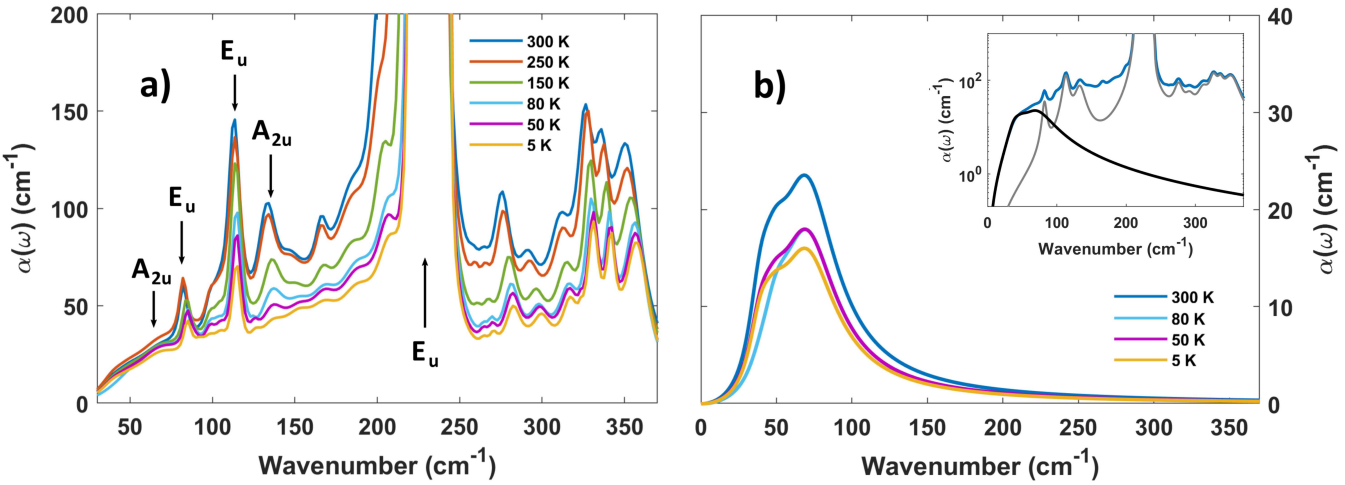

FIG. 3: | **Temperature dependence of the far infrared vibrational modes of CrI_3. a)** Absorption coefficient at various temperatures as extracted from the transmittance measurements fitting process. A general transparency is observed with decreasing temperatures, along with the disappearance of three modes at very low temperatures. The arrows highlight the main vibrational modes predicted in accordance with the D_{3d} point group symmetry. **b)** Absorption spectrum after removing the predicted in-plane phonon resonances and the few major peaks lacking a clear identification, as computed by the best fitting process of the transmittance. A general absorptive background is highlighted across the low energy spectrum, showing an increasing transparency with the lowering temperature. Visible differences in the absorption background behavior can be highlighted while crossing the Curie temperature. The inset shows the contribution of the absorbtive background (black curve) to the total absorption coefficient at 300 K (blue curve). The gray curve shows the contributions coming from the known phonon peaks.

electron-phonon interaction, whose intensity is measured by the coefficient V, higher than the one found in most of the known semiconductors (see Table I). The further blue shift of the electronic band gap below the Curie temperature (nearly 350 cm^{-1} between the actual gap value at 5 K and that extrapolated from the fitting result), suggests a further dependence of the electronic gap from the magnetic degrees of freedom. Indeed, lattice structure modifications seems to be absent across the transition, as confirmed by the nearly constant phonon spectrum (see below). However, the magnitude of the observed optical-gap energy-shift across the ferromagnetic transition cannot be simply related to any magnetic energy scale. These results suggest that the electronic gap hardening should be related to nontrivial electron-magnetic interactions[24,27,29,33], leading to a complex picture of the CrI_3 material equilibrium response.

	$E_g(0)$ **(eV)**	ϵ **(meV)**	**V**
CrI_3 (paramagnetic)	1.26	26	4.68
$CuGaS_2$[51]	2.5	38	1.53
$CdGeP_2$[50]	1.89	-	3.2
$CdGeAs_2$[50]	0.595	-	1.27
$ZnSnSb_2$[50]	0.66	-	3.74
Ge[49]	0.74	-	2.77
Si[49]	1.17	-	2.74
GaAs[49]	1.52	-	3.14

TABLE I: Coefficients for the band gap frequency shift of semiconductors as a function of temperature, as obtained by the model of eq. 1. The symbol "-" highlights missing values from literature. The resulting temperature dependence for CrI_3 is shown in fig. 2.

B. Far Infrared Response

The far-IR absorption coefficients at different temperatures are shown in Fig. 3a in an expanded vertical scale. The spectra are composed by several peaks located between 70 and 360 cm^{-1} and we observe an overall decrease of the absorption by reducing T. Due to the van der Waals nature of the CrI_3 crystal and the in-plane polarization of the incident radiation in this experiment, a single layer model for the lattice vibrations is expected to describe the experimental phonon absorption peaks. Indeed, CrI_3 layers can be described by the D_{3d} point group symmetry[29,52], which predicts five IR-allowed transitions, namely three E_u modes and two A_{2u} modes, three inactive modes (one A_{1u} and two A_{2g}), and six Raman-active modes (two A_{1g} and four E_g). Raman spectra at room-T have already been measured in pre-

vious works and the corresponding peaks are reported in Table II together with numerical calculations (at 0 K)[53–55] and the IR absorption peaks observed at room-T in our experiment, as measured by absorption peak maxima. In the theoretical calculation, the heavier iodine atoms are predicted to dominate the phonon spectrum below 150 cm^{-1}[29,56], therefore being related to the strong absorption peaks at 82 and 114 cm^{-1} (E_u modes) and 133 cm^{-1} (A_{2u} mode). At higher energies, above the strong absorption at 230 cm^{-1} (E_u symmetry, mainly due to Cr vibrations), a series of peaks can be seen in Fig. 3a, with a strong spectral weight from 300 to 360 cm^{-1}. These higher frequency excitations are not predicted by the ab-initio calculations for CrI_3[29,53,56]. However, their frequencies can be captured by a linear combination of Raman and IR fundamental modes as reported in Table II, suggesting an important role of anharmonicity in the phonon spectrum of CrI_3. Further differences from the D_{3d} point group symmetry predictions can be found in the presence of extra absorption shoulders at nearly 100, 150, 170 cm^{-1} and near the strong E_u peak at 230 cm^{-1}. The presence of these excitations has been investigated in recent DFT calculations of monolayer CrI_3[56], showing their dependence from the magnetic ordering. Indeed, their temperature dependence (they nearly disappear below T_c) is not trivial. A similar result is obtained for the A_{2u} predicted in-plane phonon at 133 cm^{-1} (as measured at $T = 300\ K$), which seems to disappear at low temperatures. These results have been explained in terms of a strong spin-phonon coupling[56], which predicts the appearance of a gap in the phonon density of states between the two E_u modes at 113 and 230 cm^{-1}.

The low-energy (THz) side of the absorption coefficient suggests the presence of a broad background. Its general shape and temperature dependence can be obtained by a best fitting process of the absorption coefficient at various temperatures, taking into account the phonon peaks previously discussed (see the inset of Fig. 3b for an example of fitting at 300 K). An absorption background has been observed in the THz range in α-$RuCl_3$[57]. Although strongly debated, this background has been mainly associated to Kitaev spin liquid excitations. In CrI_3, at variance with α-$RuCl_3$, this broad absorption, centered around 70 cm^{-1}, is already present at room-T and decreases with reducing T, nearly saturating below T_c (see Fig. 3a). This behavior suggests a non magnetic origin. As the CrI_3 resistivity is very high already at 300 K, this excludes electronic contributions to the THz absorption. Therefore, the broad THz background in CrI_3 is probably related to acoustic-phonon assisted absorption processes[57] or soft phonon modes of weakly coupled vdW layers. However, no information concerning such modes to date is available in these layered compounds[58].

Raman-active	**IR-active**	**IR-active (two-phonons)**
52 [50.1] (E_g)	60 [56.8] (A_{2u})	276 ($230E_u + 52E_g$)
79 [76.1] (A_{1g})	82 [80.3] (E_u)	291 ($230E_g + 60A_{2u}$)
99 [101.8] (E_g)	113 [114.3] (E_u)	310 ($230E_u + 79A_{1g}$)
105 [107.5] (E_g)	133 [133.3] (A_{2u})	326 ($230E_u + 99E_g$)
128 [129] (A_{1g})	230 [225.3] (E_u)	337 ($230E_u + 105E_g$)
230 [241.1] (E_g)		347 ($230E_g + 113E_u$)

TABLE II: CrI_3 vibrational modes frequencies (in cm^{-1}) at 300 K. The values in the quadratic brackets highlight the in-plane Raman- and IR-active modes at 0 K, as obtained by DFT results[29]. The first column shows the experimental Raman modes[54,55]. The IR-active experimental modes obtained in this work are shown in the second and third columns.

III. CONCLUSIONS

In this work we have investigated the optical response of a CrI_3 single crystal from Terahertz to Near-Infrared at various temperatures, both in the paramagnetic and ferromagnetic phase. We have observed an insulating optical gap around 1.1 eV at 300 K which strongly depends on temperature, showing a robust hardening for decreasing T. This hardening is due to a huge electron-phonon interaction which is reinforced below the Curie critical temperature at nearly 60 K. This indicates a complex interaction scenario among lattice, electronic and magnetic degrees of freedom in CrI_3 system.

By studying the far-IR/THz absorption spectrum we have observed several phonon peaks that have been assigned in agreement to the D_{3d} point group symmetry and DFT calculations. Our finding of some magnetic-sensitive peaks could be the first experimental evidence that these lowest-frequency absorptive terms exhibit strong spin-phonon coupling. The phonons absorption is also superimposed to a broad background already visible at 300 K and having a decreasing magnitude with T. This is at variance with the isostructural α-$RuCl_3$ compound, where the absorption background increases at low-T and has been associated mainly to Kitaev spin liquid excitations. Although CrI_3 has been suggested to be a candidate to host similar fractionalizated excitations, as indicated by recent theoretical results[59] and by the discovery of gapped Dirac magnon dispersions[41], this absorption background could have a different origin probably related to soft interlayer modes or acoustic-phonon assisted absorption processes. In conclusion, the present experiment clarifies the low-energy electrodynamics of bulk CrI_3, fixing a solid point for the investigation of its optical behavior in the dimensionality crossover from 3D to 2D.

IV. METHODS

A. Sample Growth

CrI_3 single crystals were synthesized by a chemical vapor transport technique. A 1 g mixture of the stoichiometric ratio of Cr metal and I_2 pieces (Alfa Aesar, 99.99%) was packed in a sealed evacuated quartz glass tube (22 cm long and 16 mm wide) and heated in a three zone furnace, set at zone temperatures 650, 550, and 600 °C, for one week. The "charge" was placed in the 650 °C zone. Many CrI_3 crystals were formed in the 550 °C zone. The crystals are stable in air for a few hours.

B. Optical Characterization

Optical measurements at various temperatures have been performed through a Bruker Vertex 70v Infrared interferometer, coupled with different detectors and beamsplitters covering the spectral region from THz (20 cm^{-1}) to NIR (15000 cm^{-1}). A liquid He-cooled bolometer has been used for measurements from 20 cm^{-1} up to 600 cm^{-1}, while a room-temperature pyroelectric detector has been used for the higher frequencies. The optical measurements have been taken at various temperatures through a He-cooled ARS cryostat.

* Corresponding author: stefano.lupi@roma1.infn.it

V. REFERENCES

[1] Wang, Q. H., Kalantar-Zadeh, K., Kis, A., Coleman, J. N. & Strano, M. S. Electronics and optoelectronics of two-dimensional transition metal dichalcogenides. *Nature Nanotechnology* **7**, 699–712 (2012)

[2] Manzeli, S., Ovchinnikov, D., Pasquier, D., Yazyev, O. V. & Kis, A. 2D transition metal dichalcogenides. *Nature Reviews Materials* **2**, 17033 (2017)

[3] Reedijk, J. & Poeppelmeier, K. Comprehensive Inorganic Chemistry II: From Elements to Applications, Elsevier (2013)

[4] Liu, C. W., Östling, M. & Hannon, J. B. New materials for post-Si computing. *MRS Bulletin* **39**, 658–662 (2014)

[5] Lemme, M. C., Li, L.-J., Palacios, T. & Schwierz, F. Two-dimensional materials for electronic applications. *MRS Bulletin* **39**, 711–718 (2014)

[6] Radisavljevic, B., Radenovic, A., Brivio, J., Giacometti, V. & Kis, A. Single-layer MoS_2 transistors. *Nature Nanotechnology* **6**, 147–150 (2011)

[7] Mak, K. F. & Shan, J. Photonics and optoelectronics of 2D semiconductor transition metal dichalcogenides. *Nature Photonics* **10**, 216–226 (2016)

[8] Felser, C., Fecher, G. H. & Balke, B. Spintronics: A Challenge for Materials Science and Solid-State Chemistry. *Angewandte Chemie* **46**, 5, 668-699 (2007)

[9] Schaibley, J. R. et al. Valleytronics in 2D materials. *Nature Reviews Materials* **1**, 16055 (2016)

[10] Dillon Jr., J. F., Kamimura, H., & Remeika, J. P. Magneto-optical properties of ferromagnetic chromium trihalides. *Journal of Physics and Chemistry of Solid* **27**, 9, 1531-1549 (1966)

[11] Wang, H., Eyert, V. & Schwingenschlögl, U. Electronic structure and magnetic ordering of the semiconducting chromium trihalides $CrCl_3$, $CrBr_3$, and CrI_3. *J. Phys.: Condens. Matter* **23**, 116003 (2011)

[12] Niu, B. et al. Coexistence of Magnetic Orders in Two-Dimensional Magnet CrI_3. *Nano Lett.* **20**, 1, 553–558 (2020)

[13] Pollini, I. Electron correlations and hybridization in chromium compounds. *Solid State Communications* **106**, 8, 549-554 (1998)

[14] Bermudez, V. M. & McClure, D. S. Spectroscopic studies of the two-dimensional magnetic insulators chromium trichloride and chromium tribromide—I. *Journal of Physics and Chemistry of Solids* **40**, 2, 129-147 (1979)

[15] Jin, W. et al. Observation of the polaronic character of excitons in a two-dimensional semiconducting magnet CrI_3. *Nature Communications* **11**, 4780 (2020)

[16] Tokura, Y., Yasuda, K. & Tsukazaki, A. Magnetic topological insulators. *Nature Reviews Physics* **1**, 126-143 (2019)

[17] Chang, C.-Z. et al. Experimental Observation of the Quantum Anomalous Hall Effect in a Magnetic Topological Insulator. *Science* **340**, 6129, 167-170 (2013)

[18] Jackeli, G. & Khaliullin, G. Mott Insulators in the Strong Spin-Orbit Coupling Limit: From Heisenberg to a Quantum Compass and Kitaev Models. *Phys. Rev. Lett.* **102**, 017205 (2009)

[19] Knolle, J., Kovrizhin, D. L., Chalker, J. T. & Moessner, R. Dynamics of a Two-Dimensional Quantum Spin Liquid: Signatures of Emergent Majorana Fermions and Fluxes. *Phys. Rev. Lett.* **112**, 207203 (2014)

[20] Pershan, P. S. Magneto-Optical Effects. *Journal of Applied Physics* **38**, 1482 (1967)

[21] Freiser, M. A survey of magnetooptic effects. *IEEE Transactions on Magnetics* **4**, 2 (1968)

[22] Haider, T. A Review of Magneto-Optic Effects and Its Application. *International Journal of Electromagnetics and Applications* **7**, 1, 17-24 (2017)

[23] Seyler, K. L. et al. Ligand-field helical luminescence in a 2D ferromagnetic insulator. *Nature Physics* **14**, 277–281 (2018)

[24] Liu, Z. et al. Observation of nonreciprocal magnetophonon effect in nonencapsulated few-layered CrI_3. *Science Advances* **6**, 43, eabc7628 (2020)

[25] Liu, Y. et al. Thickness-dependent magnetic order in CrI_3 single crystals. *Scientific Reports* **9**, 13599 (2019)

[26] Huang, B. et al. Layer-dependent ferromagnetism in a van der Waals crystal down to the monolayer limit. *Nature* **546**, 270–273 (2017)

[27] Gudelli, V. K. & Guo, G.-Y. Magnetism and magneto-optical effects in bulk and few-layer CrI_3: a theoretical GGA + U study. *New Journal of Physics* **21**, 053012 (2019)

[28] McGuire, M. A., Dixit, H., Cooper, V. R. & Sales, B. C. Coupling of Crystal Structure and Magnetism in the

Layered, Ferromagnetic Insulator CrI_3. *Chem. Mater.* **27**, 2, 612–620 (2015)
[29] Webster, L., Liang, L. & Yan, J.-A. Distinct spin–lattice and spin–phonon interactions in monolayer magnetic CrI_3. *Phys. Chem. Chem. Phys.* **20**, 23546-23555 (2018)
[30] Zhang, Y. et al. Switchable magnetic bulk photovoltaic effect in the two-dimensional magnet CrI_3. *Nature Communications* **10**, 3783 (2019)
[31] Bacaksiz, C., Šabani, D., Menezes, R. M. & Milošević, M. V. Distinctive magnetic properties of CrI_3 and $CrBr_3$ monolayers caused by spin-orbit coupling. *Phys. Rev. B* **103**, 125418 (2021)
[32] Chen, L. et al. Magnetic anisotropy in ferromagnetic CrI_3. *Physical Review B* **101**, 134418 (2020)
[33] Stavropoulos, P. P., Liu, X. & Kee, H.-Y. Magnetic anisotropy in spin-3/2 with heavy ligand in honeycomb Mott insulators: Application to CrI_3. *Physical Review Research* **3**, 013216 (2021)
[34] Sun, Z. et al. Giant nonreciprocal second-harmonic generation from antiferromagnetic bilayer CrI_3. *Nature* **572**, 497–501 (2019)
[35] Pervishko, A. A. et al. Localized surface electromagnetic waves in CrI_3-based magnetophotonic structures. *Optics Express* **28**, 20, 29155-29165 (2020)
[36] Tokura, Y., Kawasaki, M. & Nagaosa, N. Emergent functions of quantum materials. *Nature Physics* **13**, 1056–1068 (2017)
[37] Keimer, B. & Moore, J. E. The physics of quantum materials. *Nature Physics* **13**, 1045–1055 (2017)
[38] Nasu, J., Knolle, J., Kovrizhin, D. L., Motome, Y. & Moessner, R. Fermionic response from fractionalization in an insulating two-dimensional magnet. *Nature Physics* **12**, 912–915 (2016)
[39] Sandilands, L. J., Tian, Y., Plumb, K. W., Kim, Y.-J. & Burch, K. S. Scattering Continuum and Possible Fractionalized Excitations in α-$RuCl_3$. *Phys. Rev. Lett.* **114**, 147201 (2015)
[40] Wang, Z. et al. Magnetic Excitations and Continuum of a Possibly Field-Induced Quantum Spin Liquid in α-$RuCl_3$. *Phys. Rev. Lett.* **119**, 227202 (2017)
[41] Chen, L. et al. Topological Spin Excitations in Honeycomb Ferromagnet CrI_3. *Phys. Rev. X* **8**, 041028 (2018)
[42] Costa, A. T., Santos, D. L. R., Peres, N. M. R. & Fernandez-Rossier, J. Topological magnons in CrI_3 monolayers: an itinerant fermion description. *2D Mater.* **7**, 045031 (2020)
[43] Wu, Z., Yu, J. & Yuan, S. Strain-tunable magnetic and electronic properties of monolayer CrI_3. *Phys. Chem. Chem. Phys.* **21**, 7750-7755 (2019)
[44] Kuzmenko, A. B. Kramers-Kronig constrained variational analysis of optical data. *Review of Scientific Instruments* **76**, 083108 (2005)
[45] Freda, M. et al. Transmittance Fourier Transform Infrared Spectra of Liquid Water in the Whole Mid-Infrared Region: Temperature Dependence and Structural Analysis. *Applied Spectroscopy* **59**, 9, 1155-1159 (2005)
[46] Jung, Y., Zhou, Y. & Cha, J. J. Intercalation in two-dimensional transition metal chalcogenides. *Inorg. Chem. Front.* **3**, 452-463 (2016)
[47] Ghobadi, N. Band gap determination using absorption spectrum fitting procedure. *International Nano Letters* **3**, 2 (2013)
[48] Manoogian, A. & Woolley, J. C. Temperature dependence of the energy gap in semiconductors. *Canadian Journal of Physics* **62**, 3 (1984)
[49] Van Zeghbroeck, B. V. Principles of semiconductor devices and heterojunctions. Upper Saddle River, Pearson Education (2010)
[50] Bhosale, J. et al. Temperature dependence of band gaps in semiconductors: Electron-phonon interaction. *Phys. Rev. B* **86**, 195208 (2012)
[51] Levcenco, S. et al. Temperature dependence of the exciton gap in monocrystalline $CuGaS_2$. *Physica B: Condensed Matter* **405**, 17, 3547-3550 (2010)
[52] Bermudez, V. M. Unit-cell vibrational spectra of chromium trichoride and chromium tribromide. *Solid State Communications* **19**, 8, 693-697 (1976)
[53] Larson, D. T. & Kaxiras, E. Raman spectrum of CrI_3: An ab initio study. *Phys. Rev. B* **98**, 085406 (2018)
[54] Ubrig, N. et al. Low-temperature monoclinic layer stacking in atomically thin CrI_3 crystals. *2D Mater.* **7**, 015007 (2020)
[55] McCreary, A. et al. Distinct magneto-Raman signatures of spin-flip phase transitions in CrI_3. *Nature Communications* **11**, 3879 (2020)
[56] Wang, K. et al. Magnetic order-dependent phonon properties in 2D magnet CrI_3. *Nanoscale*, Advance Article (2021)
[57] Little, A. et al. Antiferromagnetic Resonance and Terahertz Continuum in α-$RuCl_3$. *Phys. Rev. Lett.* **119**, 227201 (2017)
[58] Reschke, S. et al. Electronic and phonon excitations in α-$RuCl_3$, *Phys. Rev. B* **96**, 165120 (2017)
[59] Xu, C., Feng, J., Xiang, H. & Bellaiche, L. Interplay between Kitaev interaction and single ion anisotropy in ferromagnetic CrI_3 and $CrGeTe_3$ monolayers. *npj Computational Materials* **4**, 57 (2018)

VI. AUTHOR CONTRIBUTIONS

All authors contributed extensively to the work presented in this paper.
L.T. and S.L. designed the experiment. S.L. and R.J.C. supervised the work. R.J.C. and L.T.N. prepared the samples. L.T., A. G., M. C. G, L. M. and S.M. measured the optical transmittance and reflectance. L.T. analyzed the data. L.T. and S.L. prepared the original draft. All authors reviewed and edited the manuscript.
All authors have read and agreed to the published version of the manuscript.

VII. FUNDING

The crystal growth, performed at Princeton University, was supported by the US Department of Energy, Division of Basic Energy Sciences, grant DG-FG02-98ER45706.

VIII. COMPETING INTERESTS STATEMENT

The authors declare no competing interests.